

Article

Kinetics and Mechanism of Aniline and Chloroanilines Degradation Photocatalyzed by Halloysite-TiO₂ and Halloysite-Fe₂O₃ Nanocomposites

Beata Szczepanik ^{1,*} , Piotr Słomkiewicz ¹ , Dariusz Wideł ¹, Marianna Czaplicka ² and Laura Frydel ¹

¹ Institute of Chemistry, Jan Kochanowski University, 7 Uniwersytecka, 25-406 Kielce, Poland; piotr.slomkiewicz@ujk.edu.pl (P.S.); dariusz.widel@ujk.edu.pl (D.W.); laura.frydel@gmail.com (L.F.)

² Institute of Environmental Engineering, Polish Academy of Sciences, 34 M. Skłodowskiej-Curie Str., 41-819 Zabrze, Poland; marianna.czaplicka@ipis.zabrze.pl

* Correspondence: beata.szczepanik@ujk.edu.pl; Tel./Fax: +48-413497028

Abstract: The kinetics of photocatalytic degradation of aniline, 2-chloroaniline, and 2,6-dichloroaniline in the presence of halloysite-TiO₂ and halloysite-Fe₂O₃ nanocomposites, halloysite containing naturally dispersed TiO₂, Fe₂O₃, commercial TiO₂, P25, and α-Fe₂O₃ photocatalysts, were investigated with two approaches: the Langmuir–Hinshelwood and first-order equations. Adsorption equilibrium constants and adsorption enthalpies, photodegradation rate constants, and activation energies for photocatalytic degradation were calculated for all studied amines photodegradation. The photodegradation mechanism was proposed according to organic intermediates identified by mass spectrometry and electrophoresis methods. Based on experimental results, it can be concluded that after 300 min of irradiation, aniline, 2-chloro-, and 2,6-dichloroaniline were completely degraded in the presence of used photocatalysts. Research results allowed us to conclude that higher adsorption capacity and immobilization of TiO₂ and Fe₂O₃ on the halloysite surface in the case of halloysite-TiO₂ and halloysite-Fe₂O₃ nanocomposites significantly increases photocatalytic activity of these materials in comparison to the commercial photocatalyst: TiO₂, Fe₂O₃, and P25.

Keywords: photodegradation; TiO₂-, Fe₂O₃-halloysite nanocomposites; aniline; chloroanilines kinetics



Citation: Szczepanik, B.; Słomkiewicz, P.; Wideł, D.; Czaplicka, M.; Frydel, L. Kinetics and Mechanism of Aniline and Chloroanilines Degradation Photocatalyzed by Halloysite-TiO₂ and Halloysite-Fe₂O₃ Nanocomposites. *Catalysts* **2021**, *11*, 1548. <https://doi.org/10.3390/catal11121548>

Academic Editor:
Hideyuki Katsumata

Received: 22 November 2021
Accepted: 15 December 2021
Published: 19 December 2021

Publisher's Note: MDPI stays neutral with regard to jurisdictional claims in published maps and institutional affiliations.



Copyright: © 2021 by the authors. Licensee MDPI, Basel, Switzerland. This article is an open access article distributed under the terms and conditions of the Creative Commons Attribution (CC BY) license (<https://creativecommons.org/licenses/by/4.0/>).

1. Introduction

Aniline and its derivatives are toxic and hardly degradable environmental pollutants [1–3]. Their widespread use in the world industry causes them to be found frequently in both effluents and surface water [2–4]. Hence, these compounds are considered to be an increasing threat to both the environment and human health. Aniline is classified as a persistent organic pollutant by the European Economic Community and US Environmental Protection Agency [5]. Therefore, it is important to use appropriate methods of removing these compounds from wastewater. There has been a great interest in technology based on the oxidation of the hazardous and refractory organic pollutants, by the use of advanced oxidation processes (AOPs) [6]. Hydroxyl radicals (HO•) as the principal agents responsible for the oxidation of numerous organic contaminants are generated in AOPs with various combinations of hydrogen peroxide, ozone, and ultraviolet light. Technology utilizing illuminated semiconductors is commonly known as the heterogeneous photocatalysis [7,8].

The photodegradation of several aniline derivatives with the use of TiO₂ was successfully applied by researchers [9–12]. Irradiation of TiO₂(anatase) with wavelengths λ < 400 nm (irradiation with sufficient energy to equal or exceed the band-gap of the semiconductor) in the presence of H₂O and O₂, adsorbed on the TiO₂ surface illustrates that there are a number of processes in which the oxidative species such as HO• and O₂•, HO₂•, and H₂O₂ are generated. The radicals are immediately involved in secondary processes in which organic pollutants adsorbed on the TiO₂ surface are oxidized [12]. Organic

pollutants, which include aniline and its derivatives, absorb UV radiation and may be photodegraded in the environment to form some poisonous intermediate products. Thus, it is important to investigate photodegradation mechanisms of organic compounds in detail. Heterogeneous photocatalysis employing TiO₂ and UV light is a promising route for the degradation of persistent organic pollutants. In addition, it produces more degradable and less-toxic substances [10,11].

The use of TiO₂ nanopowders in a solution is difficult due to the possibility of agglomeration of the photocatalyst and the problem with its recovery. Despite the fact that TiO₂ is considered a material of very low toxicity [13], studies of the risk of using this material are beginning to emerge [14]. TiO₂ nanoparticles can be released into the environment during the production and the use and/or storage of materials containing this material [15]. For this reason, the use of nanocomposites containing properly comminuted and immobilized TiO₂ nanoparticles on the surface of an appropriate carrier prevents the release of these nanoparticles into the environment [16]. Natural clay minerals are sufficient as carrier materials due to their high specific surface area, large pore volumes, chemical stability, good mechanical properties, availability, and low cost [17]. Clay minerals, such as kaolinite, rectorite, hectorite, saponite, montmorillonite, palygorskite, allophane and imogolite, have found application as carriers of TiO₂ nanoparticles, which allow us to obtain composites with high photocatalytic activity and offer the possibility of easy separation of the photocatalyst from the aqueous solution [18]. In the field of environmental catalysis, halloysite-based nanocomposites have many advantages, such as simple recovery, high yields and selectivities, and working in mild experimental conditions [19,20].

In our previous work, we prepared TiO₂- and Fe₂O₃- halloysite nanocomposites using acid-treated halloysite from Poland [21]. Chemical and phase composition, particle morphology, and physical properties of these nanocomposites were characterized. We proved the photocatalytic activities of these nanocomposites for aniline, 2-chloro-, and 2,6-dichloroaniline degradation under UV irradiation. The TiO₂- and Fe₂O₃-halloysite nanocomposites showed significantly higher photocatalytic activity in decomposing aniline and its chlorine derivatives than that of the commercial photocatalysts TiO₂ and P25.

The main objective of the present study is an analysis of photodegradation kinetics for aniline and its chlorine derivatives in aqueous solutions using UV/halloysite- TiO₂ and halloysite-Fe₂O₃ systems. Also, a degradation mechanism of aniline and its derivatives is proposed according to identified organic intermediates.

2. Results and Discussions

2.1. Kinetics

The mechanism of organic compounds photodegradation in the presence of TiO₂ consists of three steps: adsorption of compound on the surface of TiO₂, photodegradation of organic pollutant on the surface, and desorption of products of photodegradation from this surface [22]. The determination of organic compound photodegradation rate constants requires the knowledge of the adsorption constants of this compound on the photocatalyst surface.

In general, the kinetics of photocatalytic reactions of most organic compounds, including aniline and chloroanilines, are described by pseudo first-order decay kinetics rationalized in terms of the Langmuir–Hinshelwood model [12,22,23]. In this study, two assumptions were made for the course of the photocatalytic reaction kinetic for the photodegradation of aniline, 2-chloro-, and 2,6-dichloroaniline.

The first approach takes photochemical reaction in the solution into account in addition to the photocatalytic photodegradation reaction on the catalyst. It can be assumed that the photocatalytic degradation of aniline, 2-chloroaniline, and 2,6-dichloroaniline is a pseudo first-order reaction as a resultant process of these two reactions.

Pseudo first-order kinetic equation has the following form:

$$\frac{C}{C_0} = e^{-kt} \quad (1)$$

where: C —reagent concentration at time t (mg/dm^3), C_0 —initial reagent concentration (mg/dm^3), k —reaction rate constant (min^{-1}), t —irradiation time (min).

The correlation of the experimental points with the curves, determined by fitting the pseudo first-order equation by the least squares method to the results of measurements of the photodegradation reaction of aniline, 2-chloroaniline and 2,6-dichloroaniline on all used photocatalysts, is presented in Figure 1.

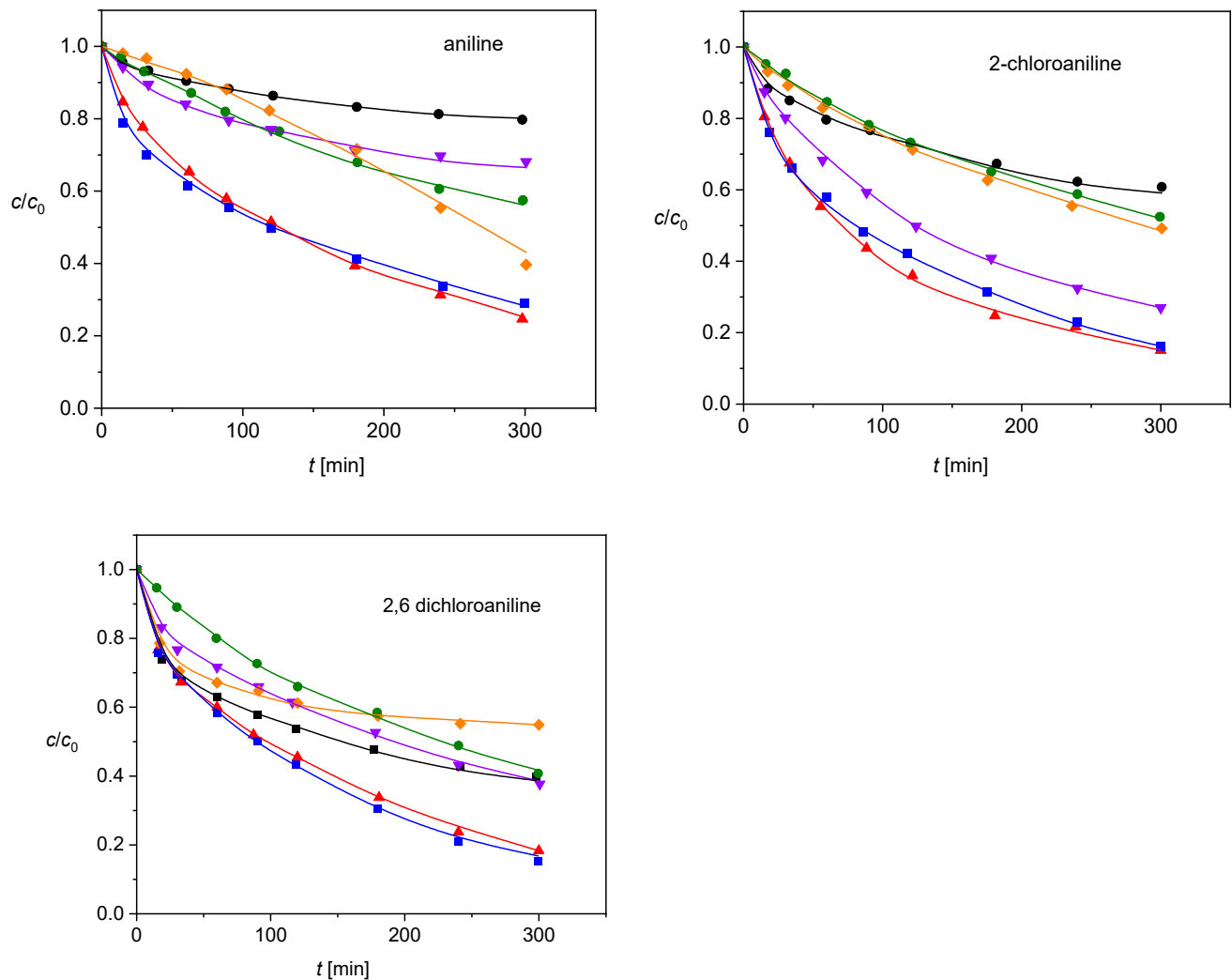


Figure 1. Correlation of experimental points with the curves determined by fitting the pseudo first-order equation by the least squares method to measurement results of the photodegradation reaction of aniline, 2-chloroaniline, and 2,6-dichloroaniline on photocatalysts: ●—P25; ▲—Hal-TiO₂; ■—Hal-Fe₂O₃; ▼—Hal; ◆—TiO₂; ●—Fe₂O₃.

Tables 1 and 2 present the results of calculations of the reaction rate constants in the kinetic Equation (1) by non-linear regression analysis, using the Origin program by Microcal [24]. These data show that the highest pseudo first-order rate constants were obtained for the Hal-TiO₂ and Hal-Fe₂O₃ nanocomposites for the photocatalytic degradation of each amine.

Table 1. Rate constant of aniline, 2-chloroaniline, and 2,6-dichloroaniline photodegradation on photocatalysts: P25; Hal-TiO₂; Hal-Fe₂O₃; Hal; TiO₂, and Fe₂O₃ at 298 K in the pseudo first-order equation adjusted to results of kinetic measurements calculated by the Levenberg–Marquardt least squares method.

Parameter	P25	Hal-TiO ₂	Hal-Fe ₂ O ₃	Hal	TiO ₂	Fe ₂ O ₃
	Aniline					
Rate constant of reaction k [min ⁻¹]	2.12×10^{-3}	1.14×10^{-2}	1.28×10^{-2}	3.75×10^{-3}	5.78×10^{-3}	4.81×10^{-3}
Error	7.69×10^{-5}	1.91×10^{-4}	3.44×10^{-4}	1.4×10^{-4}	2.09×10^{-4}	1.01×10^{-4}
Chi-Square Minimization (χ^2)	0.0012	0.0075	0.0244	0.0043	0.0090	0.0021
Regression Coefficient (R ²)	0.7938	0.9657	0.8477	0.8778	0.9084	0.9540
2-chloroaniline						
Rate constant of reaction k [min ⁻¹]	4.63×10^{-3}	1.61×10^{-2}	1.88×10^{-2}	1.10×10^{-2}	5.71×10^{-3}	5.27×10^{-3}
Error	1.83×10^{-4}	3.80×10^{-4}	3.34×10^{-4}	1.95×10^{-4}	5.90×10^{-5}	5.83×10^{-5}
Chi-Square Minimization (χ^2)	0.0069	0.0299	0.0230	0.0078	7.23×10^{-4}	7.05×10^{-4}
Regression Coefficient (R ²)	0.74535	0.9281	0.93283	0.9626	0.9881	0.9868
2,6-dichloroaniline						
Rate constant of reaction k [min ⁻¹]	8.68×10^{-3}	1.39×10^{-2}	1.51×10^{-2}	8.18×10^{-3}	6.20×10^{-3}	7.05×10^{-3}
Error	4.37×10^{-4}	2.78×10^{-4}	2.47×10^{-4}	2.17×10^{-4}	4.14×10^{-4}	6.70×10^{-5}
Chi-Square Minimization (χ^2)	0.0396	0.0160	0.0126	0.0097	0.0355	9.31×10^{-4}
Regression Coefficient (R ²)	0.8225	0.9479	0.9669	0.9008	0.84448	0.9901

Table 2. Activation energy and rate constants of aniline, 2-chloroaniline, and 2,6-dichloroaniline photodegradation on photocatalysts: P25; Hal-TiO₂; Hal-Fe₂O₃; Hal; TiO₂, and Fe₂O₃ in in the pseudo first-order equation at the range of temperature 303–323 K.

Temperature [K]	P25	Hal-TiO ₂	Hal-Fe ₂ O ₃	Hal	TiO ₂	Fe ₂ O ₃
	Aniline					
Rate Constant of Reaction k [min ⁻¹]						
303	2.62×10^{-3}	1.15×10^{-2}	1.47×10^{-2}	3.77×10^{-3}	6.40×10^{-3}	5.53×10^{-3}
313	3.59×10^{-3}	1.44×10^{-2}	1.54×10^{-2}	4.57×10^{-3}	7.38×10^{-3}	6.40×10^{-3}
323	4.63×10^{-3}	2.07×10^{-2}	2.15×10^{-2}	6.70×10^{-3}	9.38×10^{-3}	8.13×10^{-3}
Activation Energy [kJ/mol]	24.7	19.5	15.1	18.7	15.0	16.1
Temperature [K]	2-chloroaniline					
	Rate constant of reaction k [min ⁻¹]					
303	6.67×10^{-3}	2.12×10^{-2}	2.21×10^{-2}	1.34×10^{-2}	6.89×10^{-3}	6.11×10^{-3}
313	8.31×10^{-3}	2.40×10^{-2}	2.60×10^{-2}	1.52×10^{-2}	8.65×10^{-3}	7.48×10^{-3}
323	9.61×10^{-3}	2.71×10^{-2}	2.82×10^{-2}	1.78×10^{-2}	9.82×10^{-3}	8.73×10^{-3}
Activation Energy [kJ/mol]	21.7	15.1	12.6	14.4	19.3	15.9
Temperature [K]	2,6-dichloroaniline					
	Rate constant of reaction k [min ⁻¹]					
303	1.08×10^{-2}	1.61×10^{-2}	1.88×10^{-2}	9.79×10^{-3}	7.24×10^{-3}	8.85×10^{-3}
313	1.41×10^{-2}	1.95×10^{-2}	2.36×10^{-2}	1.43×10^{-2}	1.07×10^{-2}	1.17×10^{-2}
323	1.77×10^{-2}	2.72×10^{-2}	3.11×10^{-2}	1.88×10^{-2}	1.35×10^{-2}	1.50×10^{-2}
Activation Energy [kJ/mol]	22.4	20.8	22.2	26.9	25.5	23.3

The values of rate constants determined by both methods are slightly higher for 2-chloro- and 2,6-dichloroaniline than for aniline on Hal-TiO₂ and Hal-Fe₂O₃ photocatalysts. It is consistent with the higher reactivity of ortho-substituted anilines and phenols [25].

The second approach involves the Langmuir–Hinshelwood mechanism in which surface photodegradation reaction limits the overall rate of the process, which can be written in a general form [26]:

$$r = \frac{(\text{kinetic term}) (\text{driving force})}{(\text{adsorption term})^n} \quad (2)$$

Kinetic term includes kinetic constant of limiting step and adsorption equilibrium constants. The driving force is expressed analogously to homogeneous reactions in terms of concentrating the reagents. Adsorption term is characterized by the degree of surface coverage with reagents. It contains the concentration of reagents and the equilibrium constants of adsorption. Exponent n denotes the number of active sites involved in the limiting stage.

Development method of kinetics measurements, called the method of additional adsorption measurements, was proposed in Ref. [27]. This method requires supplementing kinetic measurements with measurements using the inversion liquid chromatography technique to determine the equilibrium constants for aniline, 2-chloroaniline, and 2,6-dichloroaniline adsorption on selected photocatalysts. The values of the adsorption equilibrium constants can be inserted into the Langmuir–Hinshelwood equation, which reduces the number of constants in this equation that must be calculated to fit the equation to the experimental points. The adsorption mechanism of aniline and its chlorinated derivatives was the subject of our previous research [28–30]. The Langmuir adsorption equation was determined on the basis of the analyses carried out by the inversion liquid chromatography method using the peak partitioning method [27]. After determining the parameters of the adsorption processes of aniline and chloroanilines, it was found that adsorption takes place at many active centers on the photocatalyst surface without dissociation of amine molecules. Due to the complicated surface morphology of halloysite photocatalysts, this is a great simplification, because adsorption of the adsorbate can occur simultaneously according to various mechanisms. Langmuir adsorption Equation (3) takes the form given below:

$$a = \frac{K_L C^{1/n}}{1 + K_L C^{1/n}} \quad (3)$$

where: a —adsorption capacity of adsorbent (mg/g), K_L —adsorption equilibrium constant (dm³/mg)^{1/ n} , C —concentration of adsorbate in aqueous phase (mg/dm³), n —the number of active centers.

The values of adsorption equilibrium constants for aniline, 2-chloroaniline, and 2,6-dichloroaniline on photocatalysts: P25; Hal-TiO₂; Hal-Fe₂O₃; Hal; TiO₂, and Fe₂O₃ calculated in the range of temperatures from 298 K to 323 K are presented in Table 3.

Table 3. Adsorption equilibrium constants of aniline, 2-chloroaniline, and 2,6-dichloroaniline and adsorption enthalpy on photocatalysts: P25; Hal-TiO₂; Hal-Fe₂O₃; Hal; TiO₂ and Fe₂O₃.

Temperature [K]	P25	Hal-TiO ₂	Hal-Fe ₂ O ₃	Hal	TiO ₂	Fe ₂ O ₃
	Aniline					
	Adsorption Equilibrium Constant K [dm ³ /mol]					
298	7.00×10^{-3}	1.20×10^{-2}	3.01×10^{-2}	1.60×10^{-2}	6.00×10^{-3}	2.78×10^{-2}
303	6.35×10^{-3}	1.06×10^{-2}	2.79×10^{-2}	1.52×10^{-2}	5.05×10^{-3}	2.54×10^{-2}
313	5.17×10^{-3}	9.46×10^{-3}	2.43×10^{-2}	1.37×10^{-2}	3.85×10^{-3}	2.07×10^{-2}
323	4.21×10^{-3}	8.03×10^{-3}	2.11×10^{-2}	1.16×10^{-2}	3.37×10^{-3}	1.70×10^{-2}
<i>n</i>	1.17	1.05	1.08	1.12	1.04	1.15
Adsorption enthalpy ΔH [kJ/mol]	-16.2	-12.3	-11.3	-10.2	-18.5	-15.8
Temperature [K]	2-chloroaniline					
	Adsorption equilibrium constant K [dm ³ /mol]					
	298	3.00×10^{-3}	7.34×10^{-3}	2.77×10^{-2}	2.10×10^{-2}	1.25×10^{-2}
303	2.52×10^{-3}	6.38×10^{-3}	2.32×10^{-2}	1.90×10^{-2}	9.52×10^{-3}	2.19×10^{-2}
313	1.84×10^{-3}	4.85×10^{-3}	1.83×10^{-2}	1.49×10^{-2}	7.62×10^{-3}	1.71×10^{-2}
323	1.48×10^{-3}	3.68×10^{-3}	1.46×10^{-2}	1.24×10^{-2}	5.74×10^{-3}	1.36×10^{-2}
<i>n</i>	1.6	1.55	1.86	1.42	1.05	1.17
Adsorption enthalpy ΔH [kJ/mol]	-22.6	-22.1	-20.0	-17.1	-23.6	-21.1
Temperature [K]	2,6-dichloroaniline					
	Adsorption equilibrium constant K [dm ³ /mol]					
	298	2.00×10^{-3}	3.00×10^{-3}	9.00×10^{-3}	1.10×10^{-2}	9.72×10^{-3}
303	1.52×10^{-3}	2.43×10^{-3}	6.87×10^{-3}	9.19×10^{-3}	7.67×10^{-3}	8.06×10^{-3}
313	1.11×10^{-3}	1.82×10^{-3}	4.89×10^{-3}	6.47×10^{-3}	5.20×10^{-3}	5.39×10^{-3}
323	7.31×10^{-4}	1.23×10^{-3}	4.01×10^{-3}	5.25×10^{-3}	3.52×10^{-3}	4.09×10^{-3}
<i>n</i>	1.21	1.14	1.20	1.33	1.24	1.28
Adsorption enthalpy ΔH [kJ/mol]	-31.1	-27.8	-25.5	-24.0	-32.2	-29.9

The value of adsorption centers *n* for Hal-TiO₂, Hal-Fe₂O₃, and Hal photocatalysts are averaged due to a different number of adsorption centers on their surface. The values K_L of adsorption equilibrium constants for aniline and its derivatives are lower for the P25 photocatalyst compared to the Hal-TiO₂, Hal-Fe₂O₃, and Hal photocatalysts at temperature 298 K.

Adsorption enthalpies of aniline, 2-chloroaniline, and 2,6-dichloroaniline on photocatalysts: P25; Hal-TiO₂; Hal-Fe₂O₃; Hal; TiO₂, and Fe₂O₃ were determined from the slope of the linear form of the van't Hoff Equation (4):

$$\ln K_L = -\Delta H/RT \quad (4)$$

where: ΔH —adsorption enthalpy (kJ/mol), *T*—measured temperature (K), *R*—gas constant (J/mol K).

The values of adsorption enthalpies for aniline, 2-chloroaniline, and 2,6-dichloroaniline increase in the following order: Hal < Hal-Fe₂O₃ < Hal-TiO₂ < Fe₂O₃ < P25 < TiO₂ (Table 3).

Langmuir–Hinshelwood Equation (5) has the following form while taking into account the adsorption term:

$$r = -\frac{dC_t}{dt} = \frac{kK_L C^{1/n}}{1 + K_L C^{1/n}} \quad (5)$$

where: r —reaction rate ($\text{mg}/\text{dm}^3 \cdot \text{min}$), t —irradiation time, C_t —reagents concentration at time t (mg/dm^3), c —initial reagents concentration (mg/dm^3), k —reaction rate constant ($\text{mol}/\text{dm}^3 \text{ min}$), K_L —experimental value of adsorption equilibrium constant

An example of the correlation of experimental points with the curves determined by fitting the Langmuir–Hinshelwood Equation (5) by the least squares method [31] (Origin Microcal program [24]) to the results of measurements at temperature 298 K for aniline, 2-chloroaniline, and 2,6-dichloroaniline photodegradation on photocatalysts: P25, Hal-TiO₂, Hal-Fe₂O₃, Hal, TiO₂, and Fe₂O₃ is presented in Figure 2. The curves were adjusted by the least squares method to the kinetic data after introducing adsorption equilibrium constant into the Langmuir–Hinshelwood equation.

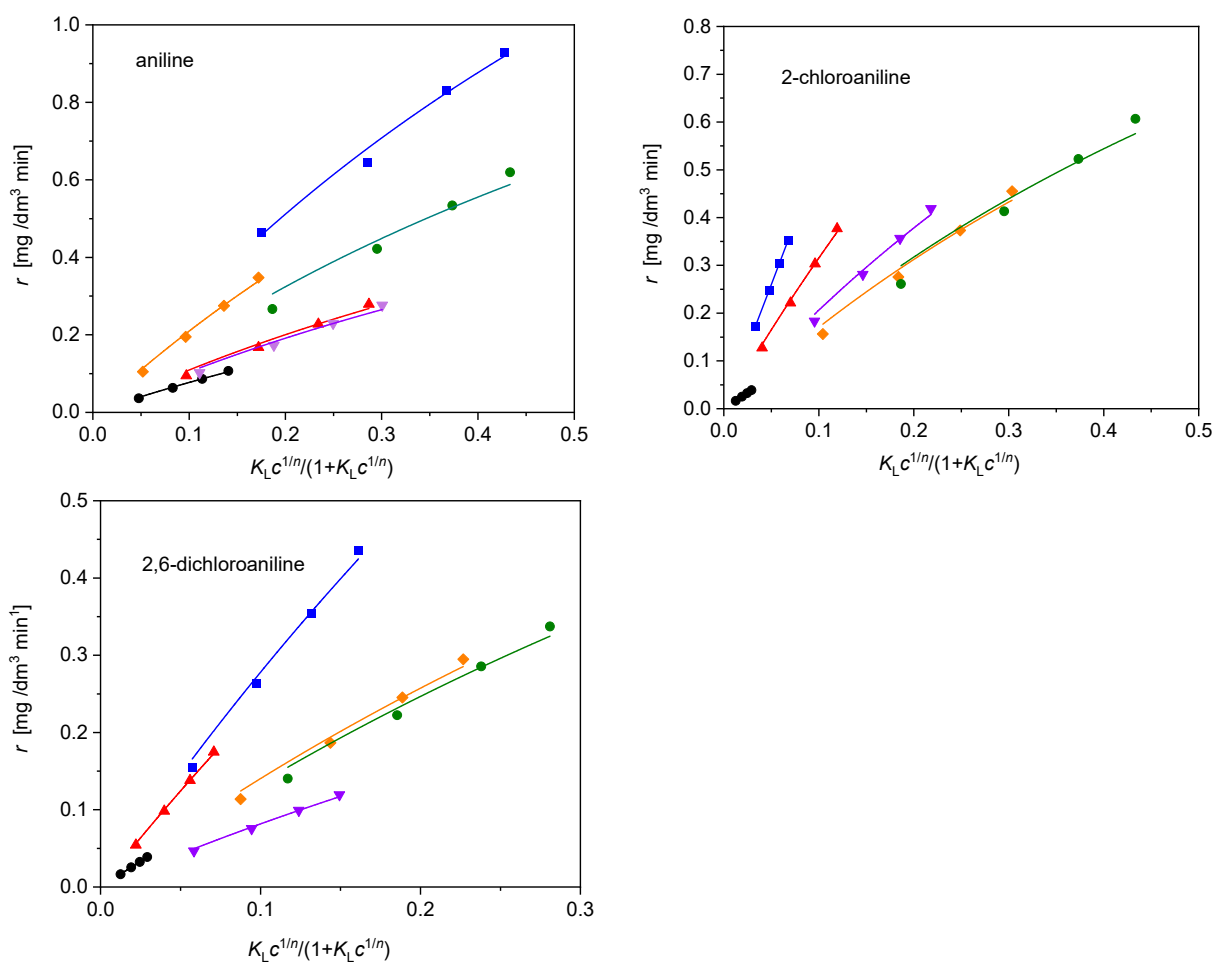


Figure 2. Correlation of experimental points with the curves determined by fitting the Langmuir–Hinshelwood equation by the least squares method to the measurement results of the photodegradation reaction of aniline, 2-chloroaniline and 2,6-dichloroaniline on photocatalysts: ●—P25; ▲—Hal-TiO₂; ■—Hal-Fe₂O₃; ▼—Hal; ◆—TiO₂; ●—Fe₂O₃.

The values of rate constants for aniline, 2-chloroaniline, and 2,6-dichloroaniline photodegradation on photocatalysts: P25; Hal-TiO₂; Hal-Fe₂O₃; Hal; TiO₂, and Fe₂O₃ obtained on the basis of the Langmuir–Hinshelwood Equation (5) for the range of temperatures 298–323 K are presented in Tables 4 and 5.

Table 4. Rate constant of aniline, 2-chloroaniline, and 2,6-dichloroaniline photodegradation on photocatalysts: P25; Hal-TiO₂; Hal-Fe₂O₃; Hal; TiO₂, and Fe₂O₃ at 298 K 298K in the Langmuir–Hinshelwood equation, adjusted to results of kinetic measurements calculated by the Levenberg–Marquardt least squares method.

Parameter	P25	Hal-TiO ₂	Hal-Fe ₂ O ₃	Hal	TiO ₂	Fe ₂ O ₃
	Aniline					
Rate constant of reaction k [mol/dm ³ min]	0.84	1.20	3.06	1.14	2.30	1.94
Error	0.0120	0.0317	0.1044	0.0305	0.0405	0.0642
Chi-Square Minimization (χ^2)	4.90×10^{-6}	1.62×10^{-4}	1.21×10^{-4}	1.20×10^{-4}	7.59×10^{-4}	1.0×10^{-3}
Regression Coefficient (R^2)	0.9947	0.9816	0.9596	0.9787	0.9930	0.9569
2-chloroaniline						
Rate constant of reaction k [mol/dm ³ min]	1.36	3.47	5.50	2.26	1.87	1.90
Error	0.0039	0.0425	0.0329	0.0427	0.0515	0.0629
Chi-Square Minimization (χ^2)	2.95×10^{-8}	4.49×10^{-5}	1.10×10^{-5}	1.47×10^{-4}	3.37×10^{-4}	9.59×10^{-4}
Regression Coefficient (R^2)	0.9996	0.99611	0.9981	0.9857	0.9796	0.9569
2,6-dichloroaniline						
Rate constant of reaction k [mol/dm ³ min]	1.35	2.61	3.05	0.89	1.54	1.48
Error	0.0039	0.002	0.0484	0.0128	0.03194	0.03541
Chi-Square Minimization (χ^2)	2.95×10^{-8}	3.68×10^{-6}	1.02×10^{-4}	6.50×10^{-6}	8.33×10^{-5}	1.51×10^{-4}
Regression Coefficient (R^2)	0.9996	0.9986	0.9929	0.9933	0.9863	0.9789

Table 5. Activation energy and rate constants of aniline, 2-chloroaniline, and 2,6-dichloroaniline photodegradation on photocatalysts: P25; Hal-TiO₂; Hal-Fe₂O₃; Hal; TiO₂, and Fe₂O₃ in in the Langmuir–Hinshelwood equation, at the range of temperature 303–323 K.

Temperature [K]	P25	Hal-TiO ₂	Hal-Fe ₂ O ₃	Hal	TiO ₂	Fe ₂ O ₃
	Aniline					
Rate constant of reaction k [mol/dm ³ min]						
303	1.03	1.40	3.61	1.30	2.54	2.19
313	1.31	1.74	4.10	1.67	2.94	2.58
323	1.79	2.15	4.61	2.01	3.39	3.02
Activation Energy [kJ/mol]	23.5	18.3	12.4	17.2	12.2	13.8
2-chloroaniline						
Rate constant of reaction k [mol/dm ³ min]						
303	1.58	4.00	6.18	2.56	2.00	2.07
313	1.96	4.67	7.01	2.99	2.45	2.54
323	2.49	5.27	7.78	3.38	2.91	3.02
Activation Energy [kJ/mol]	19.0	13.1	10.7	12.6	14.5	15.0
2,6-dichloroaniline						
Rate constant of reaction k [mol/dm ³ min]						
303	1.67	3.26	3.52	1.22	2.09	1.78
313	2.17	3.96	4.34	1.63	2.68	2.39
323	2.71	4.93	5.43	2.01	3.28	2.95
Activation Energy [kJ/mol]	21.6	19.4	18.1	25.0	23.0	22.0

Based on Figure 2 and the data contained in Table 4, it can be seen that the best correlation of the experimental points with the curves was obtained for 2-chloroaniline and 2,6-dichloroaniline. Comparing the calculation errors, function minimization values χ^2 , and regression coefficients, the best data agreement was obtained for each of the studied compounds for the P25 photocatalyst. The data in Table 4 shows that the rate constants are in each case higher when using the Hal-TiO₂ and Hal-Fe₂O₃ nanocomposites in the photocatalytic degradation of aniline, 2-chloro-, and 2,6-dichloroaniline compared to the P25 photocatalyst. This confirms high photocatalytic activity of the obtained halloysite photocatalysts.

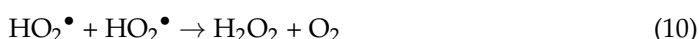
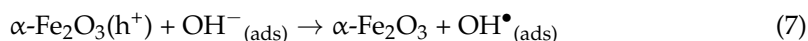
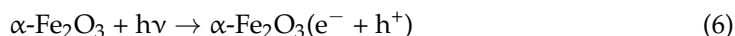
The values of activation energies for photocatalytic degradation were calculated on the basis of data collected in Tables 2 and 5 for both approaches. They are in the same order for aniline: Hal-Fe₂O₃ \approx TiO₂ < Fe₂O₃ < Hal < Hal-TiO₂ < P25. For 2-chloroaniline and 2,6-dichloroaniline, differences appear in the following order: Hal-Fe₂O₃ < Hal < Hal-TiO₂ < TiO₂ < Fe₂O₃ < P25 (first approach), and Hal-Fe₂O₃ < Hal < Hal-TiO₂ < Fe₂O₃ < TiO₂ < P25 (second approach), and for 2,6-dichloroaniline: Hal-Fe₂O₃ < Hal-TiO₂ < P25 < Fe₂O₃ < TiO₂ < Hal (first approach), Hal-TiO₂ < Hal-Fe₂O₃ < P25 < Fe₂O₃ < TiO₂ < Hal (second approach). The photodegradation activation energy values are the smallest for aniline on Hal-Fe₂O₃, for 2-chloroaniline on Hal-Fe₂O₃, and for 2,6-dichloroaniline on Hal-Fe₂O₃ and Hal-TiO₂ (Tables 2 and 5).

2.2. The Photodegradation Mechanism

The mechanism of organic-compound photodegradation in the presence of TiO₂ starts from the excitation of the titanium dioxide by a UV light wavelength ($\lambda \leq 400$ nm), which produces the photoinduced electrons and positive holes. Positive holes can be the oxidizing species during the photodegradation. Alternatively, it can react with OH[−] and H₂O molecules to produce \bullet OH radicals. In addition, the photoinduced electrons can react with electron acceptors, such as O₂ dissolved in water, to produce superoxide radical anions. All these oxidants are responsible for the photodegradation of many organic compounds. The \bullet OH species are well known to oxidize a large number of organic pollutants, including chlorinated phenols and anilines [32–34] according to the following scheme:



For α -Fe₂O₃, as in the case of TiO₂, the photodegradation mechanism also begins with the radiation absorption with energy equal to the energy of the band gap in the range of visible radiation up to 600 nm (approx. 40% of the sunlight energy), or higher than this energy. Generation of hole and excited electron are also observable. Subsequent reactions lead to forming the superoxide radical anion O₂^{•−}, the hydroperoxide radical (HO₂[•]), and the hydroxyl radical (\bullet OH) (Equations (6)–(10)) [35].



Hydroxyl radicals, electron holes, superoxide anion radicals, hydroperoxide radicals, and hydrogen peroxide, formed after radiation absorption by titanium (IV) and iron (III) oxides, are highly reactive and can oxidize aniline and its chlorine derivatives in aqueous solutions. Initial oxidation of amines is mostly a surface process, because the hydroxyl radicals might migrate only few atomic distances from the photocatalyst surface [9].

Irradiation of aniline aqueous solutions with UV radiation using TiO₂ as a photocatalyst leads to the formation of, among others, phenol, 2-aminophenol, hydroquinone, and

nitrobenzene as intermediates [36], which confirms the participation of hydroxyl radicals in the photodegradation of aniline (Figure 3) [32]. When the photodegradation process is continued long enough, these products decompose into simple inorganic ions, such as NO_2^- , NO_3^- and NH_4^+ , as well as CO_2 , and H_2O . During the photocatalytic degradation of aniline in aqueous solutions in the presence of $\alpha\text{-Fe}_2\text{O}_3$, azobenzene was found as the main intermediate product [35].

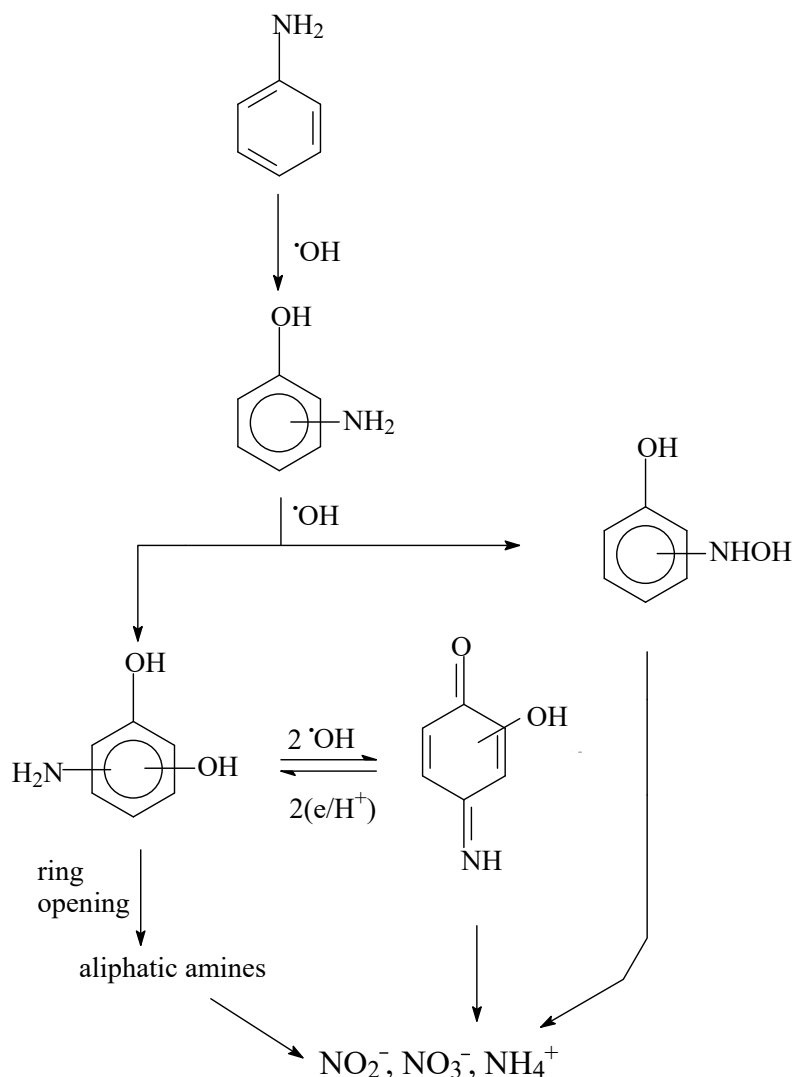


Figure 3. Mechanism of aniline photodegradation in an aqueous solution in the presence of TiO_2 .

The examination of TiO_2 -catalyzed photodegradation of 2-chloroaniline in an aqueous solution [37] showed that 2-chlorophenol and *p*-benzoquinone were the main intermediate products. In the case of photodegradation of 4-chloroaniline in the presence of TiO_2 3-hydroxy-4-chloronitrobenzene, 4-hydroxynitrobenzene, phenol, and aniline were identified as the intermediate products [38]. The photodecomposition of this amine in the $\text{TiO}_2/\text{H}_2\text{O}_2$ system leads to aniline, 4-chlorophenol, 4-chloronitrobenzene, 4-aminophenol, and 4,4'-dichloroazobenzene acting as aromatic intermediates. All these products can be oxidized to benzoquinone, which can be transformed into carboxylic acids and finally, ionic products such as Cl^- , NO_3^- , and NH_4^+ are formed [12].

Our experiments of the irradiation of aniline and 2-chloroaniline in the presence of halloysite (H) containing naturally dispersed TiO_2 and Fe_2O_3 , halloysite- TiO_2 (Hal- TiO_2), halloysite- Fe_2O_3 (Hal- Fe_2O_3) nanocomposites, and commercial P25 as photocatalysts allowed us to identify intermediate products formed during the degradation of these amines.

The analysis of the intermediates confirmed the presence of aminophenol as the main intermediate product ($\text{HOC}_6\text{H}_4\text{NH}_3^+$, 110 m/z) in the case of both amines for all used photocatalysts. The remaining products included: dimer ($\text{C}_6\text{H}_5\text{-NH-C}_6\text{H}_4\text{NH}_3^+$, 186 m/z), benzidine ($\text{H}_2\text{NC}_6\text{H}_4\text{-C}_6\text{H}_4\text{NH}_3^+$, 185 m/z), hydroxyazobenzene ($\text{H}_5\text{C}_6\text{N}=\text{NC}_6\text{H}_4\text{OH}$, 199 m/z), and smaller amounts of aniline oligomers, e.g., tetramer (protonated form, 370 m/z). The identified secondary products enabled us to propose a probable mechanism for the photodegradation of aniline and 2-chloroaniline presented in Figure 4.

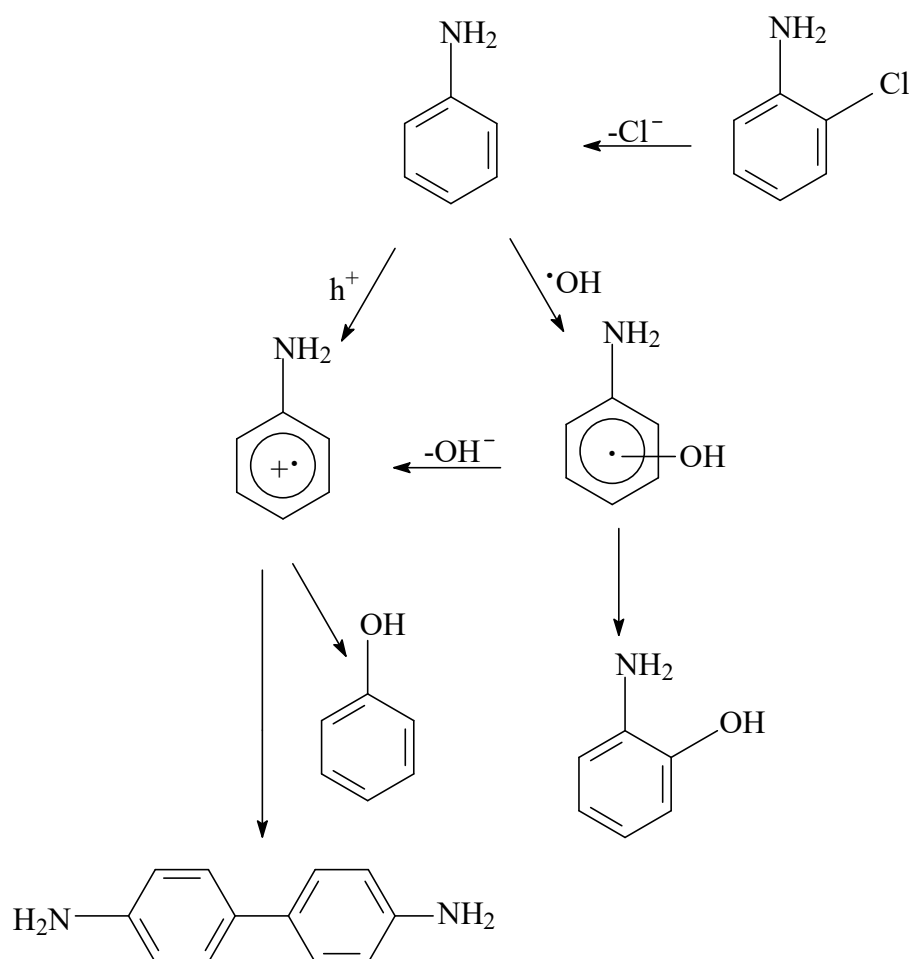


Figure 4. Mechanism of aniline and 2-chloroaniline photodegradation in an aqueous solution in the presence of halloysite- TiO_2 and halloysite- Fe_2O_3 nanocomposites, halloysite containing naturally dispersed TiO_2 and Fe_2O_3 , and commercial P25 photocatalyst.

The reaction of strongly oxidizing hydroxyl radical $\bullet\text{OH}$ with aniline molecule leads mainly to HO^\bullet -adduct, which may be transformed into 2-aminophenol or anilinium radical cation by subsequent elimination of OH^- [9]. Identifying benzidine among the intermediate products confirmed that this path of aniline transformation is probable. Aniline degradation may also result from a reaction with h^+ or $\text{HO}_2^\bullet/\text{O}_2^{\bullet-}$.

Capillary electrophoresis allowed us to determine the Cl^- and NH_4^+ ions as a final products of amine irradiation. Before sample analysis, a blind sample analysis of deionized water was performed to confirm that no ions were present in water used in the whole experiment. On the basis of the electropherogram chloride, anion was determined with a migration time of 2.721 s and an unidentified peak with migration time of 3.521 s. The second determined ion was unidentified and may be a product of the reaction with negative charge or with no electric charge. Ammonium ion was determined with migration time of 2.529 s. Determining the Cl^- and NH_4^+ ions in the solution indicated a

complete mineralization of aniline, 2-chloroaniline, 2,6-dichloroaniline, or other possible intermediate products.

3. Experimental Section

3.1. Chemicals

Halloysite was obtained from the strip mine “Dunino” (Intermark Company, Legnica, Poland). P25 titanium dioxide (Evonik, Degussa, Essen, Germany), TiO₂ (anatase), 2-chloroaniline, 2,6-dichloroaniline, (Sigma-Aldrich, Poznan, Poland) were used as received. Aniline (Aldrich) was freshly distilled under reduced pressure and stored in a refrigerator prior to use.

3.2. Preparation of Halloysite-TiO₂ and Halloysite-Fe₂O₃ Nanocomposites

The details of halloysite-TiO₂ (Hal-TiO₂) and halloysite-Fe₂O₃ (Hal-Fe₂O₃) nanocomposites synthesis and methods of their characterization were published in Ref. [21]. Experimental conditions of the preparation of these nanocomposites are collected in Table 6.

Table 6. Experimental conditions of nanocomposites preparation.

Nanocomposite	Crystallite Size	Chemicals	Conditions
Halloysite-TiO ₂	<100 nm	support-acid treated halloysite, TiO ₂ precursor-titanium tetraisopropoxide, isopropanol, HNO ₃	hydrothermal method, mixture stirred for 24 h at 65 °C
Halloysite-Fe ₂ O ₃	5–10 nm	support-acid treated halloysite, Fe ₂ O ₃ precursor-gelatinous ferric hydroxide, FeCl ₃ , deionized water	sol-gel method, mixture stirred for 24 h at 65 °C, calcination at 180 °C for 2 h

3.3. Adsorption Experiments

Inverse Liquid Chromatography (ILC) with a peak division (PD) method is a quick and accurate method to determine adsorption equilibrium constants [28]. We previously used this method [39] to calculate the adsorption equilibrium constants for aniline and 4-chloroaniline on halloysite adsorbent. In the present paper, the Langmuir equation was used to calculate equilibrium constants.

Adsorption Measurements by the PD ILC Method

A Dionex UltiMate 3000 Series chromatography system (Thermo Fisher Scientific, Inc. Waltham, MA USA), equipped with a pump, six-port injection valve, chromatographic column thermostat, and UV-Vis detector module, was used during adsorption experiments. Adsorption measurements for aniline and its chlorine derivatives were conducted with a chromatographic column (10 cm long, 0.8 mm id). The column contained about 1 g of each catalyst with a grain diameter of 0.2–0.35 mm. The column was conditioned for 1 h prior to measurement with redistilled water (0.06 µS/cm) at a flow rate of 0.5 mL/min and a pressure value of about 42 bar. Each measurement was repeated three times.

3.4. Photoreactor and Irradiation Experiments

Photodegradation experiments were carried out in a laboratory reactor—the Heraeus system—using a low-pressure mercury lamp (Figure 5). This reactor was modified by application heating jacket in order to control and stabilize the temperature and temperature meter. Reagent samples were withdrawn by syringe via a sampling connector. Prior to irradiation, photocatalyst was added to the amine solution, and the suspensions were stirred in the dark for 30 min to ensure adsorption–desorption equilibrium. The concentration amine solution in initial and irradiated samples was determined spectrophotometrically (UV-VIS-NIR UV-3600 spectrophotometer Shimadzu, Kyoto, Japan).

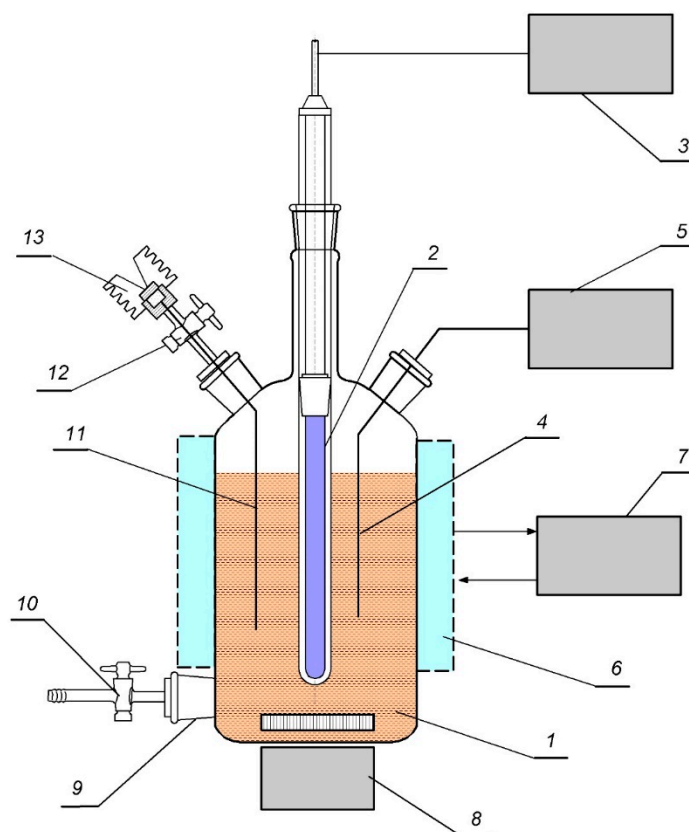


Figure 5. Scheme of photocatalytic reactor: 1–reactor, 2–UV lamp, 3–UV lamp power supply, 4–temperature sensor, 5–temperature meter, 6–heating jacket, 7–thermostat, 8–magnet stirrer, 9–outlet connector, 10–outlet valve, 11–sampling pipe, 12–sampling valve, 13–sampling connector for syringe.

Photodegradation experiments were conducted at different temperatures from 298 to 323 K. The details of these measurements are described in Ref. [21]. Experimental conditions of photocatalytic degradation of aniline, 2-chloroaniline, and 2,6-dichloroaniline are listed in Table 7. Each measurement was repeated three times.

Table 7. Experimental conditions of photocatalytic degradation of aniline, 2-chloroaniline, and 2,6-dichloroaniline.

Photocatalyst	Temperature (K)	Conditions
Halloysite-TiO ₂	298 303 313 323	Photocatalyst concentration: 2.9 g/dm ³ Initial concentration of amine: 40 mg/dm ³ Initial pH: 6 Constant stirring, time of irradiation: 300 min.
Halloysite-Fe ₂ O ₃		
P25		
TiO ₂ (anatase)		
Fe ₂ O ₃		
Halloysite (Hal)		

3.5. Product Analysis

The identification of photodegradation organic products was carried out using a Bruker Daltonik micrOTOF (time of flight) mass spectrometer (Bruker Daltonik, Bremen, Germany) using an electrospray interface equipped with an ESI interface.

The capillary electrophoresis instrument, used for selected inorganic ions determination, was a P/ACE MDQ system equipped with a UV-Vis detector (Beckman Coluter, Palo Alto, CA, USA). The fused silica capillary was of 75 μm in internal diameter and 67.2 cm

in total length (60.2 cm to detection window). The linear vertical dimension window in a capillary cartridge was 800 μm . New capillary was conditioned by washing with 1 mol/L NaOH aqueous solution (10 min), 0.1 mol/L NaOH aqueous solution (10 min) prior to first use. The sample was injected in pressure mode under 0.5 psi for 5 s. Separation conditions were as follows: 30 kV, temperature of the capillary 25 °C, detector wavelength at 200 nm for ammonium cation and 230 nm for chloride anion. At the beginning of each analysis, capillary was rinsed by 0.1 mol/L NaOH aqueous solution for 30 s, then with buffer solution for 1.0 min, and with deionized water for 1 min. The total time of the analysis was 8 min. All data were collected and analyzed with the Karat 32 software. Two sets of reagents were used for CE analyses: Anion Analysis Kit (No. A53537) and Cation Analysis Kit (No. A53540) from Analis, Namur, Belgium.

4. Conclusions

Adsorption of aniline and its chlorine derivatives on halloysite-TiO₂ and halloysite-Fe₂O₃ nanocomposites, halloysite containing naturally dispersed TiO₂ and Fe₂O₃, is more efficient than on commercial photocatalysts, as evidenced by the values of adsorption equilibrium constants higher than for TiO₂ and P25. The values of adsorption enthalpies also confirm that adsorption occurs more easily on the halloysite photocatalysts than for commercial photocatalysts.

Two models were used to describe the kinetics of the photocatalytic reaction. The first Langmuir–Hinshelwood model assumed the photodegradation of aniline, 2-chloroaniline and 2,6-dichloroaniline as a photocatalytic reaction involving a photocatalyst, ignoring the photochemical reaction. The second pseudo first-order kinetic equation took into account both photocatalytic reaction on the photocatalyst and the photochemical reaction of amines. However, comparing the results of these calculations, the values of the photodegradation rate constants calculated from both the Langmuir–Hinshelwood and the pseudo first-order equations were clearly higher for halloysite-TiO₂ and halloysite-Fe₂O₃ nanocomposites in comparison to the others photocatalysts. The higher adsorption capacity and the immobilization of TiO₂ and Fe₂O₃ on the halloysite surface significantly increases photocatalytic activity of these nanocomposites. Higher values of rate constants for chlorinated derivatives of aniline in comparison with unsubstituted aniline are associated with the presence of chlorine substituent in *ortho* position, which results in higher reactivity of these derivatives [38].

Aminophenol as the main photoproduct found upon photocatalytic degradation of aniline and chloroanilines on halloysite photocatalysts and benzidine as the minor product confirmed that the mechanism of photodegradation, is similar to the mechanism of aniline photodegradation in the presence of TiO₂ as photocatalysts. Hydroxyazobenzene detection proves the similarity of the photodegradation course, such as in the presence of α -Fe₂O₃, when azobenzene was found as the main intermediate product during the photocatalytic degradation of aniline in aqueous solution [35]. Smaller amounts of aniline oligomers, e.g., tetramers, confirm that photooxidation of aniline in the presence of photocatalysts containing TiO₂ can lead either to the photodegradation of this compound or to the effect of polymerization [40].

The presented in-depth kinetic analysis and the details of the photodegradation mechanism are important for understanding the degradation process of such pollutants as aniline and chloroanilines on halloysite catalysts. It is of great significance for the development of efficient and environmentally friendly heterogeneous photocatalyst.

Author Contributions: Investigation—B.S., L.F., D.W.; Formal analysis—P.S.; Writing original draft—B.S. and P.S.; Discussion of the results—M.C.; Writing review & editing—B.S., P.S. All authors have read and agreed to the published version of the manuscript.

Funding: This work was funded by resources of the Ministry of Science and Higher Education as research project SUPB.RN.21.188.

Conflicts of Interest: The authors declare no conflict of interest.

References

1. Chu, W.; Choy, W.K.; So, T.Y. The effect of solution pH and peroxide in the TiO₂-induced photocatalysis of chlorinated aniline. *J. Hazard. Mater.* **2007**, *141*, 86–91. [[CrossRef](#)]
2. Gosetti, F.; Chiuminatto, U.; Zampieri, D.; Mazzucco, E.; Marengo, E.; Gennaro, M.C. A new on-line solid phase extraction high performance liquid chromatography tandem mass spectrometry method to study the sun light photodegradation of mono-chloroanilines in river water. *J. Chromatogr. A* **2010**, *1217*, 3427–3434. [[CrossRef](#)]
3. Gosetti, F.; Bottaro, M.; Gianotti, V.; Mazzucco, E.; Frascarolo, P.; Zampieri, D.; Oliveri, C.; Viarenga, A.; Gennaro, M.C. Sun light degradation of 4-chloroaniline in waters and its effect on toxicity. A high performance liquid chromatography—Diode array—Tandem mass spectrometry study. *Environ. Pollut.* **2010**, *158*, 592–598. [[CrossRef](#)]
4. Jen, J.F.; Chang, C.T.; Yang, C. On-line microdialysis–high-performance liquid chromatographic determination of aniline and 2-chloroaniline in polymer industrial wastewater. *J. Chromatogr. A* **2001**, *930*, 119–125. [[CrossRef](#)]
5. Li, J.; Jin, Z. Effect of hypersaline aniline-containing pharmaceutical wastewater on the structure of activated sludge-derived bacterial community. *J. Hazard. Mater.* **2009**, *172*, 432–438. [[CrossRef](#)]
6. Azbar, N.; Yonar, T.; Kestioglu, K. Comparison of various advanced oxidation processes and chemical treatment methods for COD and color removal from a polyester and acetate fiber dyeing effluent. *Chemosphere* **2004**, *55*, 35–43. [[CrossRef](#)] [[PubMed](#)]
7. Oncescu, T.; Nitoi, I.; Oancea, P. Chlorobenzene degradation assisted by TiO₂ under UV irradiation in aqueous solutions. *J. Adv. Oxid. Technol.* **2008**, *11*, 105–110. [[CrossRef](#)]
8. Oncescu, T.; Stefan, M.; Oancea, P. Photocatalytic degradation of dichlorvos in aqueous TiO₂ suspension. *Environ. Sci. Pollut. Res.* **2010**, *17*, 1158–1166. [[CrossRef](#)]
9. Canle, M.; Santaballa, J.A.; Vuliet, E. On the mechanism of TiO₂-photocatalyzed degradation of aniline derivatives. *J. Photochem. Photobiol. A Chem.* **2005**, *175*, 192–200. [[CrossRef](#)]
10. Choy, W.K.; Chu, W. Photooxidation of *o*-chloroaniline in the presence of TiO₂ and IO₃[−]: A study of photo-intermediates and successive IO₃[−] dose. *Chem. Eng. J.* **2008**, *136*, 180–187. [[CrossRef](#)]
11. Brillas, E.; Mur, E.; Sauleda, R.; Sanchez, L.; Peral, J.; Domenech, X.; Casado, J. Aniline mineralization by AOP's: Anodic oxidation photocatalysis electro-Fenton and photoelectron-Fenton processes. *Appl. Catal. B Environ.* **1998**, *16*, 31–42. [[CrossRef](#)]
12. Nitoi, I.; Oancea, P.; Cristea, I.; Constsntin, L.; Nechifor, G. Kinetics and mechanism of chlorinated aniline degradation by TiO₂ photocatalysis. *J. Photochem. Photobiol. A Chem.* **2015**, *298*, 17–23. [[CrossRef](#)]
13. Chawengkijwanich, C.; Hayata, Y. Development of TiO₂ powder-coated food packaging film and its ability to inactivate *Escherichia coli* in vitro and in actual tests. *Int. J. Food Microbiol.* **2008**, *123*, 288–292. [[CrossRef](#)]
14. Li, S.Q.; Zhu, R.R.; Zhu, H.; Xue, M.; Sun, X.Y.; Yao, S.D.; Wang, S.L. Nanotoxicity of TiO₂ nanoparticles to erythrocyte in vitro. *Food Chem. Toxicol.* **2008**, *46*, 3626–3631. [[CrossRef](#)] [[PubMed](#)]
15. Reijnders, L. The release of TiO₂ and SiO₂ nanoparticles from nanocomposites. *Polym. Degrad. Stab.* **2009**, *94*, 873–876. [[CrossRef](#)]
16. Chorfi, H.; Zayani, G.; Saadoun, M.; Bousselmi, L.; Bessais, B. Understanding the solar photo-catalytic activity of TiO₂–ITO nanocomposite deposited on low cost substrates. *Appl. Surf. Sci.* **2010**, *256*, 2170–2175. [[CrossRef](#)]
17. Dong, Y.; Liu, Z.; Chen, L. Removal of Zn(II) from aqueous solution by natural halloysite nanotubes. *J. Radioanal. Nucl. Chem.* **2012**, *292*, 435–443. [[CrossRef](#)]
18. Szczepanik, B. Photocatalytic degradation of organic contaminants over clay-TiO₂ nanocomposites: A review. *Appl. Clay Sci.* **2017**, *141*, 227–239. [[CrossRef](#)]
19. Machado, G.S.; Castro, K.A.D.d.F.; Wypych, F.; Nakagakia, S. Immobilization of metalloporphyrins into nanotubes of natural halloysite toward selective catalysts for oxidation reactions. *J. Mol. Catal. A Chem.* **2008**, *283*, 99–107. [[CrossRef](#)]
20. Zhang, Y.; Tang, A.; Yang, H.; Ouyang, J. Applications and interfaces of halloysite nanocomposites. *Appl. Clay Sci.* **2016**, *119*, 8–17. [[CrossRef](#)]
21. Szczepanik, B.; Rogala, P.; Słomkiewicz, P.M.; Banaś, D.; Aldona Kubala-Kukuś, A.; Stabrawa, I. Synthesis, characterization and photocatalytic activity of TiO₂-halloysite and Fe₂O₃-halloysite nanocomposites for photodegradation of chloroanilines in water. *Appl. Clay Sci.* **2017**, *149*, 118–126. [[CrossRef](#)]
22. Shahrezaei, F.; Mansouri, Y.; Zinatizadeh, A.A.L.; Akhbari, A. Photocatalytic Degradation of Aniline Using TiO₂ Nanoparticles in a Vertical Circulating Photocatalytic Reactor. *Int. J. Photoenergy* **2012**, *2012*, 430638. [[CrossRef](#)]
23. Augugliaro, V.; Prevot, A.B.; Loddo, V.; Marci, G. Photodegradation kinetics of aniline, 4-ethylaniline and 4-chloroaniline in aqueous suspension of poly-crystalline titanium dioxide. *Res. Chem. Intermed.* **2000**, *26*, 413–426. [[CrossRef](#)]
24. Anonymous. *Origin User's Manual*; Microcal Software Inc.: Northampton, MA, USA, 2021.
25. Czaplicka, M.; Czaplicki, A. Photodegradation of 2,3,4,5-tetrachlorophenol in water/methanol mixture. *J. Photochem. Photobiol. A* **2006**, *178*, 90–97. [[CrossRef](#)]
26. Szarawara, J.; Skrzypek, J. *Podstawy Inżynierii Reaktorów Chemicznych*; WNT: Warszawa, Poland, 1980.
27. Słomkiewicz, P.M. Determination of the Langmuir–Hinshelwood kinetic equation of synthesis of ethers. *Appl. Clay A Gen.* **2004**, *269*, 33–42. [[CrossRef](#)]
28. Słomkiewicz, P.M.; Szczepanik, B.; Garnuszek, M.; Rogala, P.; Witkiewicz, Z. Determination of Adsorption Equations for Chloro Derivatives of Aniline on Halloysite Adsorbents Using Inverse Liquid Chromatography. *J. AOAC Int.* **2017**, *100*, 1715–1726. [[CrossRef](#)]

29. Szczepanik, B.; Słomkiewicz, P.M.; Garnuszek, M.; Czech, K. Adsorption of chloroanilines from aqueous solutions on the modified halloysite. *Appl. Clay Sci.* **2014**, *101*, 260–264. [[CrossRef](#)]
30. Szczepanik, B.; Słomkiewicz, P. Photodegradation of aniline in water in the presence of chemically activated halloysite. *Appl. Clay Sci.* **2016**, *124–125*, 31–38. [[CrossRef](#)]
31. Marquardt, D.W. An algorithm for least-squares estimation of nonlinear parameter. *J. Soc. Indust. Appl. Math.* **1963**, *11*, 431. [[CrossRef](#)]
32. Carp, O.; Huisman, C.L.; Reller, A. Photoinduced reactivity of titanium dioxide. *Prog. Solid State Chem.* **2004**, *32*, 33–177. [[CrossRef](#)]
33. San, N.; Hatipoglu, A.; Cinar, Z. Effect of molecular properties on the photocatalytic degradation rates of dichlorophenols and dichloroanilines in aqueous TiO₂ suspensions. *Toxicol. Environ. Chem.* **2004**, *86*, 145–160. [[CrossRef](#)]
34. Lindner, M.; Theurich, J.; Bahnemann, D.W. Photocatalytic degradation of organic compounds: Accelerating the process efficiency. *Water Sci. Technol.* **1997**, *35*, 79–86. [[CrossRef](#)]
35. Karunakaran, C.; Senthilvelan, S. Fe₂O₃-photocatalysis with sunlight and UV-light: Oxidation of aniline. *Electrochem. Commun.* **2006**, *8*, 95–101. [[CrossRef](#)]
36. Karunakaran, C.; Senthilvelan, S.; Karuthapandian, S. TiO₂-photocatalyzed oxidation of aniline. *J. Photochem. Photobiol. A Chem.* **2005**, *172*, 207–213. [[CrossRef](#)]
37. Choy, W.K.; Chu, W. Semiconductor-Catalyzed Photodegradation of *o*-chloroaniline: Products study and Iodate effect. *Ind. Chem. Res.* **2007**, *46*, 4740–4746. [[CrossRef](#)]
38. Devi, L.G.; Krishnamurthy, G. TiO₂- and BaTiO₃-Assisted Photocatalytic Degradation of Selected Chloroorganic Compounds in Aqueous Medium: Correlation of Reactivity/Orientation Effects of Substituent Groups of the Pollutant Molecule on the Degradation Rate. *J. Phys. Chem. A* **2011**, *115*, 460–469. [[CrossRef](#)] [[PubMed](#)]
39. Szczepanik, B.; Słomkiewicz, P.M.; Garnuszek, M. Determination of adsorption isotherms of aniline and 4-chloroaniline on halloysite adsorbent by inverse liquid chromatography. *Appl. Clay Sci.* **2015**, *114*, 221–228.
40. Tang, H.; Li, J.; Bie, Y.; Zhu, L.; Zou, J. Photochemical removal of aniline in aqueous solutions: Switching from photocatalytic degradation to photo-enhanced polymerization recover. *J. Hazard. Mater.* **2010**, *175*, 977–984. [[CrossRef](#)]